Chapter 2
Stabilisation of Clay Mixtures and Soils by Alkali Activation

Alastair Marsh, Andrew Heath, Pascaline Patureau, Mark Evernden and Pete Walker

2.1 Introduction

Alkali-activated materials (AAM) have emerged in recent decades as novel materials for several applications, including construction materials (Davidovits 2011; Provis 2014). One of their main selling points is their prospect as a low-carbon building material. This is due to their typically low curing temperature of <100 °C and also that their precursor preparation does not chemically require the release of carbon, unlike Portland cement (Heath et al. 2014; Khale and Chaudhary 2007). A geopolymer is an amorphous, alkali aluminosilicate phase that is typically produced by a dissolution–condensation reaction between an aluminosilicate precursor and an alkaline activating solution, such as a concentrated aqueous sodium hydroxide solution (Duxson et al. 2007a). The formation of a geopolymer depends on several compositional and processing conditions, including the extent of dissolution and Si:Al molar ratio of the system (Duxson et al. 2007b). Alkali activation can also produce zeolitic reaction products (Criado et al. 2007).

A. Marsh (✉)
School of Civil Engineering, University of Leeds, Leeds LS2 9JT, UK
e-mail: a.marsh@leeds.ac.uk

A. Heath · M. Evernden · P. Walker
Department of Architecture & Civil Engineering, University of Bath, Bath BA2 7AY, UK
e-mail: a.heath@bath.ac.uk

M. Evernden
e-mail: m.evernden@bath.ac.uk

P. Walker
e-mail: p.walker@bath.ac.uk

P. Patureau
Department of Chemistry, University of Bath, Bath BA2 7AY, UK
e-mail: p.m.f.patureau@bath.ac.uk

B. V. V. Reddy et al. (eds.), *Earthen Dwellings and Structures*,
Springer Transactions in Civil and Environmental Engineering,
https://doi.org/10.1007/978-981-13-5883-8_2

The aluminosilicate precursors used in AAM are commonly fly ash, blast furnace slag, other industrial by-products, metakaolin, or mixtures thereof (Pacheco-Torgal et al. 2008). Subsoil has the benefit of being a precursor that is widely available and available at very low environmental cost (Diop and Grutzeck 2008). In these systems, the clay minerals in the soil are the aluminosilicate reactant, with the other less reactive phases acting as an aggregate. Thus, the alkali aluminosilicate product phase performs the role of stabiliser for the remnant components in the soil. In effect, the clay minerals become a water-resistant binder, replacing the role of cement in a concrete block. Some researchers have investigated adding industrial by-products (e.g. fly ash) to soils before alkali activation, but this research is focussed on natural soils without any other precursors.

Soil materials stabilised by alkali activation have good environmental prospects by virtue of their low curing temperature, avoidance of chemical production of carbon during preparation and availability of subsoil (Diop and Grutzeck 2008; Murmu and Patel 2018). However, there is still a significant knowledge gap around how soil composition influences the alkali activation reaction, and in particular the reaction products formed. The mix of clay minerals in soil is of most interest, as out of the minerals typically found in soil, the clay minerals are the largest reactive components in the activation reaction (Xu and van Deventer 2000; Autef et al. 2012). The clay minerals most commonly found in soils are kaolinite, montmorillonite and illite (Nickovic et al. 2012). In this study, alkali activation was done on samples of these individual clays and also on a mixture of all three. The aim was to determine whether phase formation behaviour for the mixture differed from that expected by the behaviour of the individual clay minerals.

2.2 Materials and Methods

Imerys Speswhite kaolin (abbreviation = Kao) (mined from Cornwall, U.K.), K10 montmorillonite (abbreviation = Mont) (Sigma-Aldrich, product no. 69866-1KG) and Clay Minerals Society IMt-2 (Silver Hill) illite (abbreviation = ILL) were used as the precursor clays. The clays were activated by adding sodium hydroxide solution and mixing. The concentrations and quantities of sodium hydroxide solution were selected to give an Na:Al molar ratio of 1 for each system, whilst keeping the wet mix workability at approximately the plastic limit (Marsh et al. 2018b). The first constraint was used as a molar ratio of Na:Al = 1 is the stoichiometric balance theoretically required for geopolymer formation (Barbosa et al. 2000), the second constraint used to be compatible with extrusion processing (Maskell et al. 2013). This was achieved for all systems except the activated illite, which due to its lower plastic limit had a maximum ratio of Na:Al = 0.75.

Solutions of different concentrations were prepared by adding sodium hydroxide pellets to distilled water, mixed with a magnetic stirrer (Stuart UC152 heat-stir) for a minimum of 2 h until fully dissolved and then allowed to cool. The clays were pre-dried in a 105 °C oven and left to cool. For the mixture, the constituent clays

Table 2.1 Clay contents of the samples given in wt%

Sample	Kao content	Mont content	ILL content	[NaOH] molarity	NaOH solution: clay mass ratio
Kao-activated	100%	n/a	n/a	16.1	0.73
Mont-activated	0%	100%	n/a	6.4	0.77
ILL-activated	0%	n/a	100%	19.7	0.39
Kao-Mont-ILL-activated	33%	33%	33%	13.6	0.65

were then dry-mixed together using a magnetic stirrer for 5 min. Varying quantities of activating solutions were added to each clay or clay mixture, as given in Table 2.1. Each wet mix of activating solution and clay was mixed by hand for 3 min, providing a consistent and well-distributed mixture. The high viscosity of the samples allowed them to be compacted by hand into 18 mm × 36 mm cylindrical Teflon moulds by tamping with a glass rod in three layers for each sample, using 25 blows for each layer. Samples were cured in an air atmosphere in a 80 °C oven for 24 h in their moulds. A control sample was made for each composition, by adding distilled water and then mixing and curing in the same manner.

Activated samples of illite and 33Kao–33Mont–33ILL did not fully dry with curing, so were forcibly dried in a vacuum desiccator for 72 h.

The set of characterisations were done at 28 ± 2 days ageing time and (with the exception of SEM imaging) were done using powders prepared from the cured samples. Powders were prepared by grinding by hand, having been wetted with isopropanol to avoid damaging the clay minerals' crystal structures (Moore and Reynolds 1997). Powder X-ray diffraction (PXRD) analysis was done to identify phases with a Bruker D8 Advance instrument using monochromatic CuKα1 L3 ($\lambda =$ 1.540598 Å) X-radiation and a Vantec superspeed detector. A step size of 0.016°(2θ) and step duration of 0.3 s were used. Phase identification was done using Bruker EVA software. Scanning electron microscope (SEM) imaging was used on a fracture surface of the bulk samples sputter coated with gold for 3 min, to characterise phase size and morphology. A JEOL SEM6480LV was used in secondary electron mode with an accelerating voltage (AV) of 10 kV.

2.3 Results

2.3.1 Precursors

The PXRD patterns of the precursors are given in Fig. 2.1. The kaolinite precursor contained kaolinite clay mineral as the major phase, with muscovite and quartz present as minor phases, as expected from a Cornish residual deposit. The montmorillonite precursor contained Ca-montmorillonite clay mineral as the major phase, as well as muscovite, quartz and minor amounts of kaolinite. The illite precursor contained illite clay mineral as the major phase, with quartz, microcline and kaolinite present as minor phases. Previous studies on this source clay identified the illite clay mineral to be mostly of the 1 M/1 Md polytype (Haines and van der Pluijm 2008). Their chemical compositions are given in Table 2.2.

Table 2.2 Chemical composition of clay precursors in oxide wt%

Oxide	Al_2O_3	CaO	Fe_2O_3	K_2O	MgO	Na_2O	SiO_2	SO_3	TiO_2	Total
Kaolinite (std error)	40.11 (0.15)	0.00	0.95 (0.06)	2.06 (0.09)	0.04 (0.04)	0.00	56.83 (0.15)	0.00	0.00	100
K10 montmorillonite (std error)	13.53 (0.66)	0.47 (0.14)	4.53 (1.05)	1.56 (0.22)	1.67 (0.11)	0.03 (0.03)	77.60 (2.12)	0.12 (0.07)	0.49 (0.02)	100
Illite (std error)	20.80 (0.34)	0.00	8.32 (0.38)	8.67 (0.18)	2.28 (0.06)	0.00	59.14 (0.26)	0.00	0.78 (0.06)	100

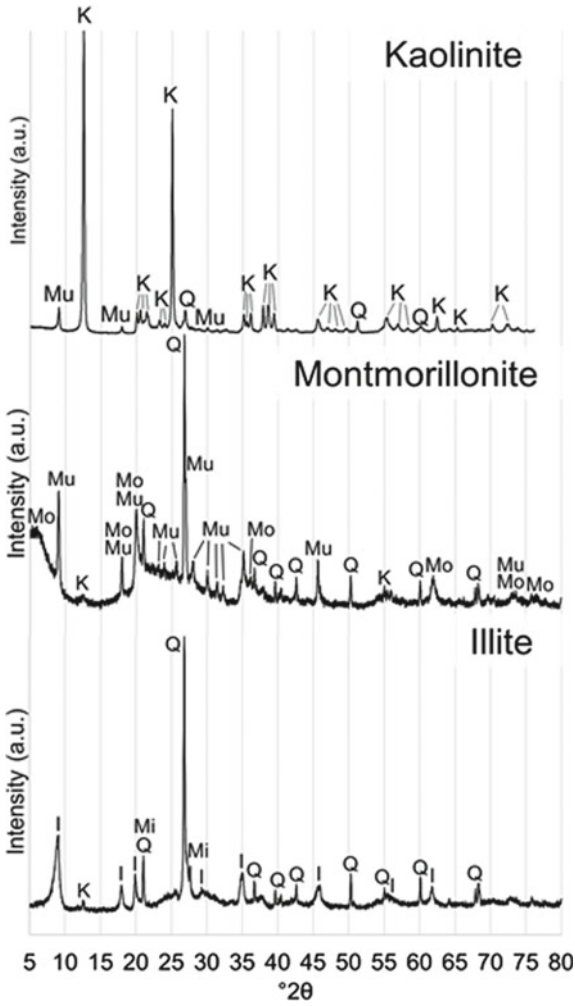

Fig. 2.1 PXRD patterns of **a** kaolinite precursor; **b** K10 montmorillonite precursor; **c** IMt-2 illite precursor. Indexed as: I = illite; K = kaolinite; Mi = microcline; Mo = montmorillonite; Mu = muscovite; Q = quartz

2.3.2 Kaolinite

Alkali activation of kaolinite produced the hydrosodalite $Na_8[AlSiO_6]_4.(OH)_2{\cdot}2H_2O$ (abbreviated as 8:2:2) as the product phase, a member of the zeolite family (Marsh et al. 2018b). This was clearly evident in the strong crystalline peaks in the PXRD pattern (Fig. 2.2), as well as the 0.5–1 μm crystallites in the SEM image (Fig. 2.3). As seen in both the XRD and SEM, a significant amount of kaolinite was consumed in the reaction, but some remained unreacted. No shrinkage was observed in the cured sample, and no unusual morphological or colour changes were observed either (Fig. 2.4).

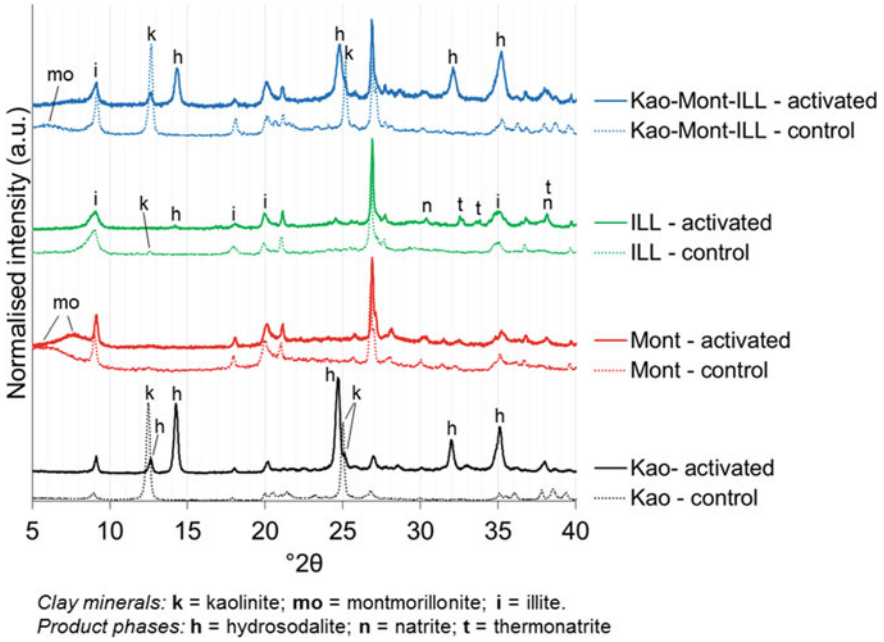

Fig. 2.2 XRD patterns of control and activated samples of kaolinite, montmorillonite, illite and a mixture of all three. For simplicity, only the clay minerals and product phases have been indexed

2.3.3 Montmorillonite

Activation of montmorillonite produced a geopolymer as the product phase. This can be seen in the PXRD pattern from the characteristic shift in the background in the region of 22–35°2θ (Duxson et al. 2007a) (Fig. 2.2). No new crystalline peaks were observed. Some of the montmorillonite clay mineral was consumed, but some remained unreacted. The 001 reflection shifted after activation, a change in d-value from 14.4 to 11.6 Å. This decrease in interlayer space was partly attributed to cation exchange of Na^+ in the sodium hydroxide activating solution for Ca^{2+} in the montmorillonite's interlayer sites (Marsh et al. 2018a). The microstructure of the activated sample was very different to that of the plate-like clay minerals in the precursor, with a semi-continuous morphology indicative of geopolymer formation (Provis et al. 2005) (Fig. 2.3). The cured sample showed very distinctive radial shrinkage cracks, aligned upwards (Fig. 2.4).

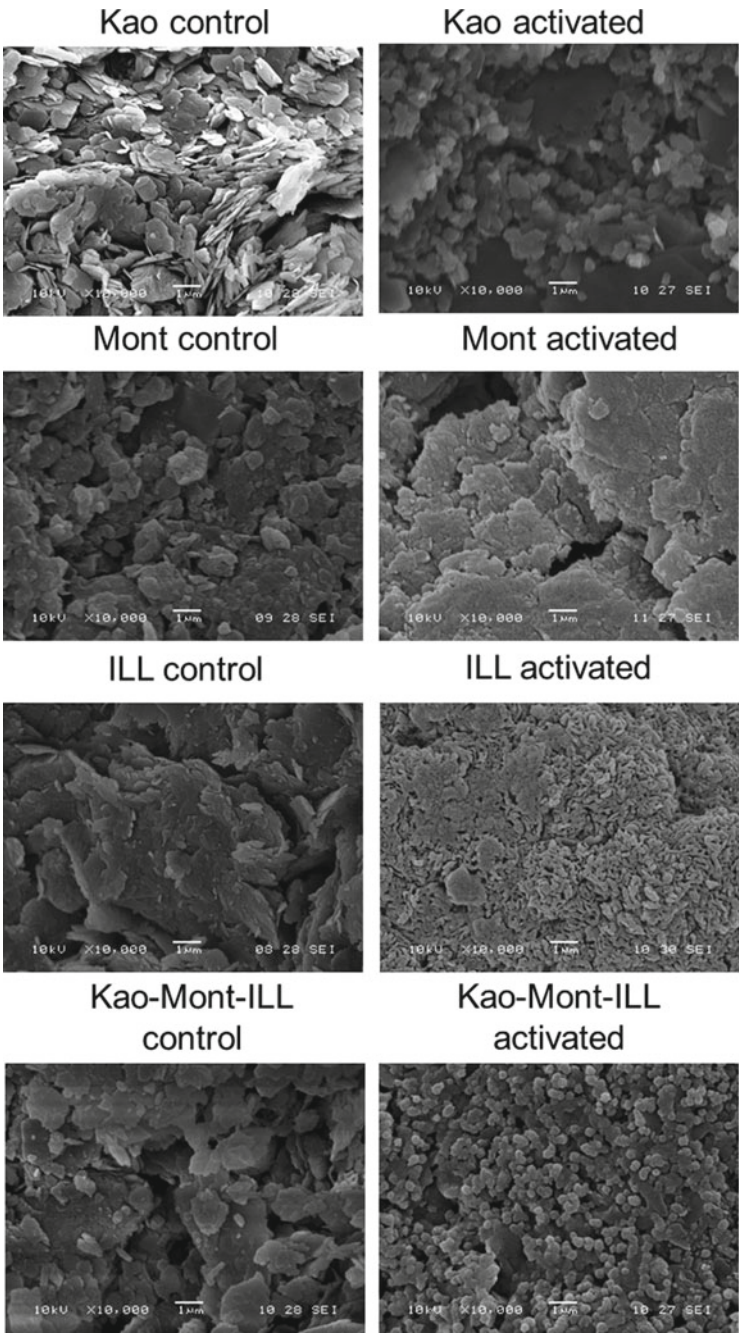

Fig. 2.3 SEM images of control and activated samples of kaolinite, montmorillonite, illite and a mixture of all three

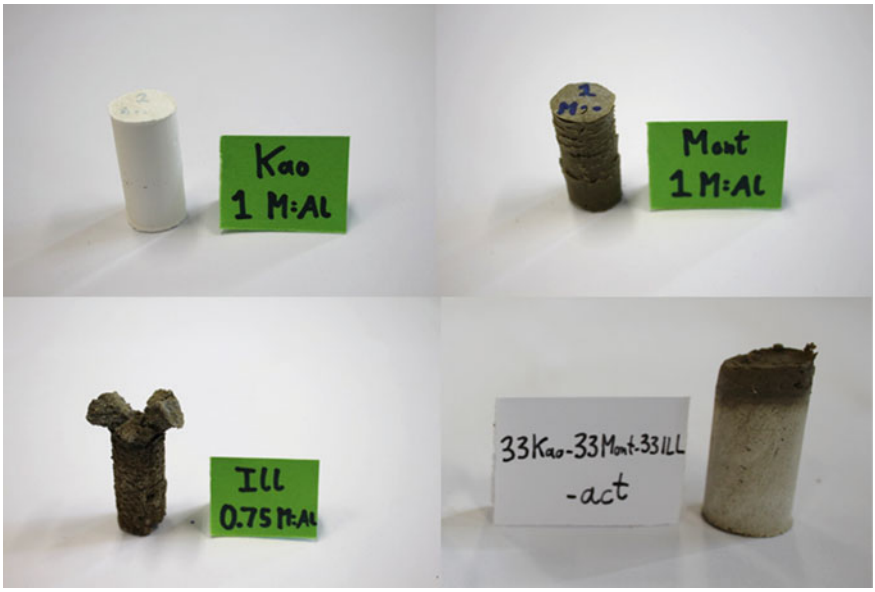

Fig. 2.4 Photographs of activated samples of kaolinite, montmorillonite, illite and a mixture of all three

2.3.4 Illite

Activation of illite did not result in a product phase, but instead resulted in the alteration of the illite clay mineral. The XRD pattern of the activated sample contained no major new crystalline peaks (Fig. 2.2), but contained minor peaks attributed to hydrosodalite, natrite (Na_2CO_3) and thermonatrite ($Na_2CO_3 \bullet H_2O$) (Marsh et al. 2018a). The microstructure of the activated illite is significantly different to the precursor, mostly due to the emergent porosity (Fig. 2.3). This porosity on the micro-scale may have contributed to the significant expansion which was observed upon curing (Fig. 2.4).

2.3.5 Kaolinite–Montmorillonite–Illite Mixture

The major reaction product was 8:2:2 hydrosodalite, as seen in the XRD pattern of the activated sample (Fig. 2.2). There was some evidence of a background shift in the region of 22–35°2θ, but not enough to conclusively show that a geopolymer was formed. None of the clay minerals in the precursors were fully consumed. Particles of ~300 nm size were observed in the SEM images of the activated sample (Fig. 2.3). No structural defects, shrinkage or expansion was observed in the cured sample, but

there was noticeable darkening around the top of the sample at the open end of the mould (Fig. 2.4).

2.4 Discussion

Using a consistent Na:Al ratio, different clay minerals have vastly different reactions to alkaline activation. Kaolinite forms hydrosodalite, a crystalline phase; montmorillonite forms a geopolymer, an amorphous phase; illite does not form a product phase, but instead seems to undergo alteration. A difference between kaolinite (a 1:1 clay) and montmorillonite (a 2:1 clay) is expected, since geopolymers are favoured over crystalline reaction products for systems with Si:Al $\geq$ 1.5 (Duxson et al. 2007b). However, the difference between the montmorillonite and illite (both 2:1 clays) suggests that alkali activation behaviour is strongly influenced by clay mineralogy rather than Si:Al stoichiometry alone.

In the test case of an equal mix of all three clay precursors, the result is not trivial to interpret. On the evidence available, the activated clay mixture is likely to contain a mix of hydrosodalite and geopolymer. Whilst geopolymers are straightforward to detect in highly reactive, simple systems such as metakaolin or fly ash, it is much more difficult in less reactive, multi-component systems such as uncalcined clay mixtures and soils. This is especially the case in low Si:Al systems where zeolitic and geopolymer reaction products can coexist (Rahier et al. 1997; Buchwald et al. 2011).

The influence of mineralogy on curing defects also opens many questions. The defects observed here are extreme, given that the clay mineral content of these samples is far higher than would ever be used in earth construction. A greater proportion of aggregate phases such as quartz would reduce the extent of these. However, it is another indication of how much there is still to be understood about these systems.

2.5 Conclusion

There are large differences in phase formation behaviour after the alkali activation of individual clay minerals. The phases formed from alkali activation of an equal mixture of these clay minerals are roughly equivalent to those formed in the individual clay minerals. Hence, it seems that the phase formation of a given clay mixture or soil could roughly be predicted from knowing the amount and types of clay minerals present. However, it also seems there is an additional degree of complexity in the phase formation behaviour of a mixture, beyond that of the individual clay minerals. This means that the exact behaviour of a given clay mixture or soil can only be fully known by testing. The findings of this study have identified an emergent issue—a greater understanding is required in order to determine how much of a difference

this additional complexity of mixtures could make to the properties of construction materials made with alkali-activated clays or soils.

References

Autef A, Joussein E, Gasgnier G, Rossignol S (2012) Role of the silica source on the geopolymerization rate. J Non-Cryst Solids 358(21):2886–2893

Barbosa VFF, MacKenzie KJD, Thaumaturgo C (2000) Synthesis and characterisation of materials based on inorganic polymers of alumina and silica: sodium polysialate polymers. Int J Inorg Mater 2:309–317

Buchwald A, Zellmann HD, Kaps C (2011) Condensation of aluminosilicate gels—model system for geopolymer binders. J Non-Cryst Solids 357(5):1376–1382

Criado M, Fernández-Jiménez A, Palomo A (2007) Alkali activation of fly ash: effect of the SiO2/Na2O ratio: Part I: FTIR study. Microporous Mesoporous Mater 106:180–191

Davidovits J (2011) Geopolymer chemistry and applications, 3rd edn. Institut Geopolymere, Saint-Quentin, Saint-Quentin

Diop MB, Grutzeck MW (2008) Low temperature process to create brick. Constr Build Mater 22:1114–1121

Duxson P, Fernández-Jiménez A, Provis JL, Lukey GC, Palomo A, van Deventer JSJ (2007a) Geopolymer technology: the current state of the art. J Mat Sci 42:2917–2933

Duxson P, Mallicoat SW, Lukey GC, Kriven WM, van Deventer JSJ (2007b) The effect of alkali and Si/Al ratio on the development of mechanical properties of metakaolin-based geopolymers. Colloids Surf, A 292:8–20

Haines SH, van der Pluijm BA (2008) Clay quantification and Ar–Ar dating of synthetic and natural gouge: application to the Miocene Sierra Mazatán detachment fault, Sonora, Mexico. J Struct Geol 30:525–538

Heath A, Paine K, McManus M (2014) Minimising the global warming potential of clay based geopolymers. J Clean Prod 78:75–83

Khale D, Chaudhary R (2007) Mechanism of geopolymerization and factors influencing its development: a review. J Mat Sci 42:729–746

Marsh A, Heath A, Patureau P, Evernden M, Walker P (2018a) Alkali activation behaviour of un-calcined montmorillonite and illite clay minerals. Applied Clay Sci 166:250–261

Marsh A, Heath A, Patureau P, Evernden M, Walker P (2018b) A mild conditions synthesis route to produce hydrosodalite from kaolinite, compatible with extrusion processing. Microporous Mesoporous Mater 264:125–132

Maskell D, Heath A, Walker P (2013) Laboratory scale testing of extruded earth masonry units. Mater Des 45:359–364

Moore DM, Reynolds RC (1997) X-ray diffraction and the identification and analysis of clay minerals, 2nd ed. Oxford, Oxford University Press

Murmu AL, Patel A (2018) Towards sustainable bricks production: an overview. Constr Build Mater 165:112–125

Nickovic S, Vukovic A, Vujadinovic M, Djurdjevic V, Pejanovic G (2012) High-resolution mineralogical database of dust-productive soils for atmospheric dust modeling. Atmos Chem Phys 12(2):845–855

Pacheco-Torgal F, Castro-Gomes J, Jalali S (2008) Alkali-activated binders: a review. Part 2. About materials and binders manufacture. Constr Build Mater 22:1315–1322

Provis JL (2014) Geopolymers and other alkali activated materials: why, how, and what? Mater Struct 47:11–25

Provis JL, Lukey GC, van Deventer JS (2005) Do geopolymers actually contain nanocrystalline zeolites? A reexamination of existing results. Chem Mater 17:3075–3085

Rahier H, Simons W, Van Mele B, Biesemans M (1997) Low-temperature synthesized aluminosilicate glasses: Part III Influence of the composition of the silicate solution on production, structure and properties. J Mat Sci 32(9):2237–2247

Xu H, Van Deventer JSJ (2000) The geopolymerisation of alumino-silicate minerals. Int J Miner Process 59(3):247–266